1 ***<u>Review paper</u>***

2 **DUMPSITE CHARACTERISATION IN EKPOMA FROM INTEGRATED SURFACE**

3 **GEOPHYSICAL METHODS**

4

5 **Abstract**

6 Foreseeable consequences of the practice of solid waste disposal in landfills are gas and leachate

7 generation due primarily to microbial decomposition, climatic conditions and refuse

8 characteristics. Hence, this paper presents an assessment of the effects of functional and an

9 abandoned waste dumpsite using Electromagnetic and electrical resistivity methods in dump

10 located along Police Barrack Road, Ekpoma in Esan West Local Government Area of Edo State.

11 Very Low Frequency - Electromagnetic (VLF-EM) field data were obtained in four traverses

12 measuring 70 m, 70 m, 40 m and 45 m at profiles 01, 02, 03 and 04, respectively. The VLF-EM

13 data were analysed through qualitative interpretation of the curves and analyzed using Karous-

14 Hjelt Software, to delineate the conductive and non-conductive zones in the study area. Four

15 Vertical Electrical Sounding (VES) stations were utilized, using Schlumberger configuration.

16 Data obtained from the (VES) technique were processed using IP2win software. The VES curves

17 obtained revealed simple subsurface geology with characteristic H and A curve types with low

18 resistivities in the range of 37.21 Ωm to 44.9 Ωm indicative of leachate contamination. The VLF

19 technique revealed lithology with high amplitudes in the region of 35 m and 40-45 m, 21-30 m

20 and 17-24 m also indicative of contamination arising from leachate wastes and underground

21 pollution in the dumpsites.

22 Keywords: landfill, solid waste disposal, biodegradation, leachate, environmental impacts,

23 Ekpoma

24 **Introduction**

25 The presence of a dumpsite in a place only implies that over time there will be dissolution of

26 solids in which chemicals are leached into the ground. The resulting leachate migrates and

27 increases the conductivity of the area in its course compared to other areas that are not affected.

28 In this vain the competence of such area is greatly compromised. Many waste dumpsites are

29 sources of environmental pollution because waste is still largely disposed without effective

30 safety and control measures. Waste dumpsites are very popular in urban or semi urban cities and

31 rural settlements alike. Wastes are defined as materials which have no further use to the owner

32 and hence disposed off [1]. The ever increasing demand for large space for domestic and
33 industrial wastes from urban areas makes them a necessary part of the human cycle of activities
34 [2]. Over the years, there has been a conservable growth in the awareness of environmental
35 pollution problems and it has become a major national and international political issue. The
36 study area along police Barrack Road Ekpoma, which lies in the guinea or derived savannah of
37 Nigeria is experiencing the problem of municipal solid waste management, principally as a result
38 of unplanned development, rural – rural migration, natural increase in population of people in the
39 areas and imprudence on the part of the engineers who dug the pit form which sand was taken
40 during the construction of truck C, Police Barrack Road a long time ago without any iota of
41 foresightedness that the particular road will be a linear settlement in the nearest future.
42 Geophysical survey was done on the dump site (Plate 1) using two geophysical methods, Direct
43 Resistivity Method and Very Low Frequency Method to access the impact of the dumpsite on its
44 environment and also to estimate the harm done to the soil so as to ascertain the competence of
45 the land for civil engineering construction and the depth of penetration of leachate from the
46 wastes due to migration and percolation. Earth materials are either resistive or conductive.
47 Materials found at dumpsites which have being infiltrated by chemical from biodegradable
48 wastes, have resistivities or conductivities greatly altered by the migrating chemicals. Since
49 direct resistivity method of electrical prospecting exploits the resistivity of the earth materials as
50 an anomaly, it is therefore one of the most suitable geophysical method for the intended study.
51 Also, Very Low Frequency Electromagnetic method exploits the conductivity contracts in each
52 materials at subsurface as anomaly-which makes it another suitable method for the proposed
53 study [3].
54

55

56   Plate 1: An overview of dumpsite at Police barrack road, Ekpoma

57   **Site Description and Geology**

58   The study area (Ekpoma) falls within the Anambra Basin. It lies approximately within Latitudes

59   6° 41' N and 6° 49' N, and Longitudes 6° 00' E and 6° 14' E (Fig. 1a & 1b) It is at a distance of

60   about 78km from Benin City [4]; [5]. The geologic formations in the area are mainly of Bende-

61   Ameki formations which consist of sandstone, clay and shale. However, there are some localize

62   places in Ekpoma that are underlain by the Ogwashi Asaba and Imo Shale Formations which

63   consist of sandstone, clay and laterites. The average annual temperature in Ekpoma is 24.8^oC.

64   Precipitation is lowest in January; with an average of 11mm. The greatest amount of

65   precipitation occurs in September, with an average of 303 mm, at an average temperature of

66   26.6^oC, March is the hottest month of the year. The lowest average temperatures in the year

67   occur in August, when it is around 23.0^oC. Between the driest and wettest months, the in

68   precipitation is 292 mm. The variation in temperatures throughout the year is 3.6^oC. Its elevation

69   ranges from 243.9 m (812 ft) to 426.6 m (1420 ft) above sea level. The predominant vegetation is

70   moist deciduous forest, which is very rich in timber resources. The canopy is more open in the

71   north than in the rain forest region which lies to the South with the tropical hard wood, timber

72   such as Iroko, Obeche *etc*. Industrial and food crops found in the area include palm oil, rubber,

73   plantain and many local important fruits strive within the forest.
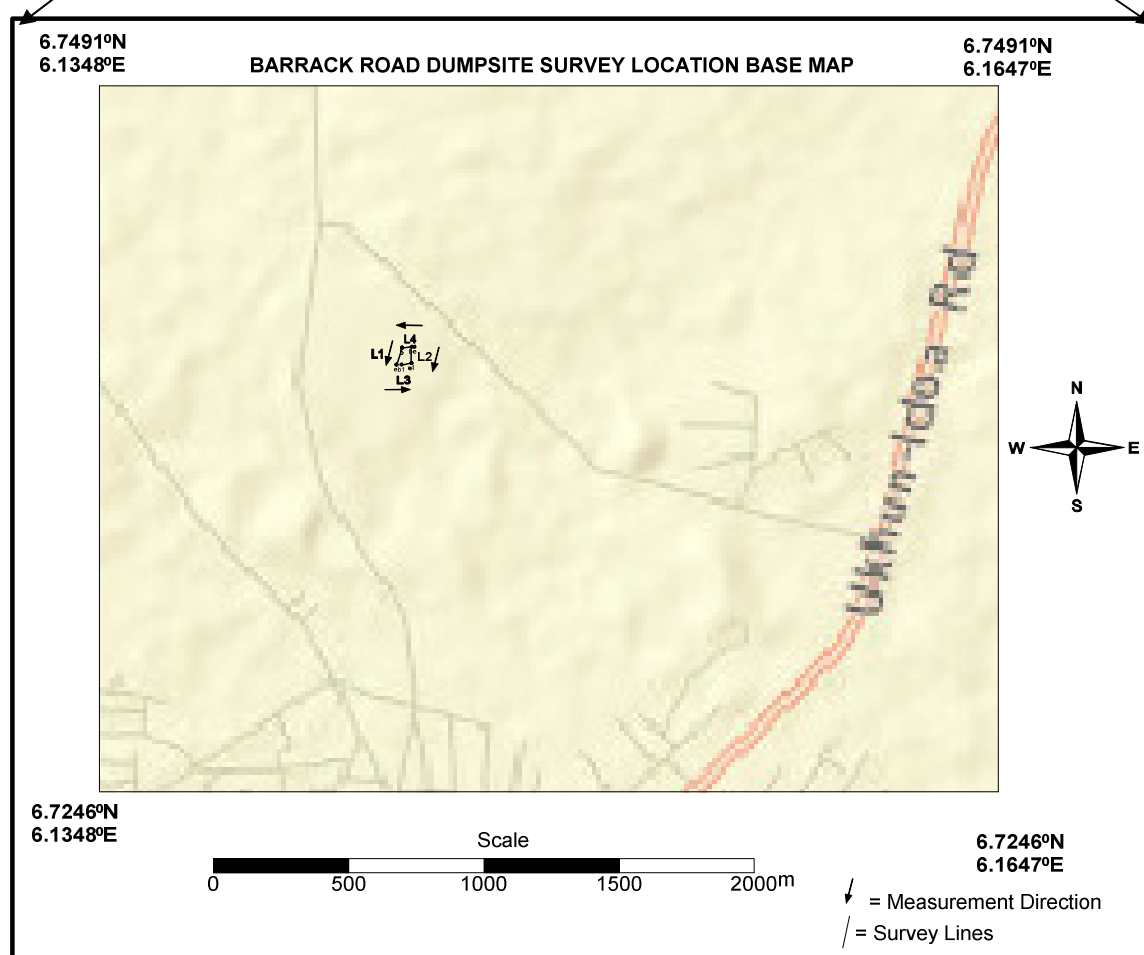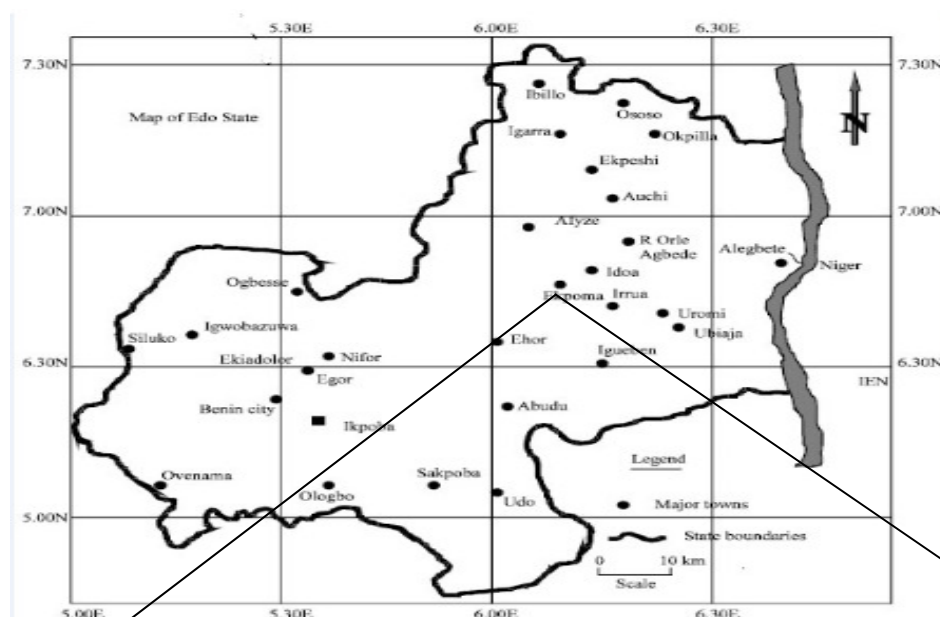
74

75

3

76

77

78

79   Fig.1: (a) Geographical map of Edo State. (b) Base map of study area Along Barrack Road.

4

80 **Materials and Methods**

81 Two geophysical methods were applied in this study.

82 **(i) VLF electromagnetic method**

83

84 The Very Low Frequency Electromagnetic (VLF-EM) method, was used because it is

85 remarkably suitable in surveying for electrical conductors by remote sensing. It has been useful

86 for ground surveying and mapping geologic formation for the past forty years [6]. VLF

87 surveying involves measurement of the earth's response to EM waves generated by transmitters

88 at remote distance from the survey site through current induction. These transmitters generate

89 plane EM waves that can induce secondary eddy currents, particularly in electrically conductive

90 elongated 2-D targets. The EM waves propagate through the subsurface and are subjected to

91 local distortions by the conductivity contracts in this medium. The subsurface occurrence of

92 these conductive bodies creates a local secondary field which has its own components.

93 Measurement of these components may be use as an indicator for locating the subsurface

94 conductive zones. The VLF-EM waves travel in three modes: skywave, spacewave (wave-guided

95 by the ionosphere and earth surface), and groundwave. As the groundwave is attenuated through

96 long distances, only the skywave and spacewave are received as the primary wave [7]. The depth

97 of penetrations of these waves depends on the frequencies and the electrical conductivity of the

98 ground in relation to skin depth. Skin depth is a measure of the penetration of electromagnetic

99 wave propagating in a conductor. Skin depth δ is a function of frequency and is given by [8] as

100
$$\delta = \left(\frac{2}{\mu\sigma\varpi} \right)^{\frac{1}{2}} \approx 500 \left(\frac{\rho}{f} \right)^{\frac{1}{2}} \tag{1}$$

101 Where; μ = Magnetic permeability of free space = $4\pi \times 10^{-7}$ Henry/m, ρ = apparent resistivity, f

102 = transmission frequency σ = conductivity and ϖ = Angular frequency ($2\pi f$).

103 At very large distances from a source of electromagnetic waves, attenuation of this type would

104 control the depth of exploration. The effective depth of exploration, Z_e, is the maximum depth

105 beneath the subsurface where a body can produce recognizable signals. By [9], it is given as

106 $$Z_e = 100 \left(\frac{\rho}{f} \right)^{\frac{1}{2}} \tag{2}$$

107   For VLF-EM, the frequencies are too high for much penetration, so that the method is useful

108   only for shallow geologic mapping. Ground VLF survey provides a quick and powerful tool for

109   the study of geological structures to a maximum skin depth of about 100 m [10] though variation

110   in the skin depth is based on changes in subsurface conductivity. VLF-EM data were collected

111   using ABEM WADI equipment, with station spacing of 5 m. The transmitter's EM wave adopted

112   has frequency of 18.8 KHz and signal strength of 13.

113   Experiments have showed that all EM phenomena are governed by empirical Maxwell's

114   equations, which are uncoupled first-order linear Partial Differential Equations (PDEs).

115   An EM field may be defined as a domain of four vector functions:

116   **e** (V/m) – electric field intensity, **b** (Wb/m^2 or Tesla) – magnetic induction,

117   **d** (C/m^2) – dielectric displacement, **h** (A/m) – magnetic field intensity.

118   All EM phenomena obey Maxwell's equations whose conventional general form in the time

119   domain is:

120     $$\nabla \wedge e + \frac{\partial b}{\partial t} = 0, \tag{3}$$

        $$\nabla \wedge h - \frac{\partial d}{\partial t} = j, \tag{4}$$

122     $$\nabla \bullet b = 0, \tag{5}$$

123     $$\nabla \bullet d = \rho, \tag{6}$$

124   Where j (A/m^2) is electric current density and ρ (C/m^3) is electric charge density. Generally

125   speaking, unconsolidated rocks are moderate conductors; and crystalline rocks are poor

126   conductors because of their lack of porosity and absence of dissolved ions and water. Qualitative

127   interpretation of VLF data is based on [11] and [12] methods. The Fraiser's operators use

128   dynamic frequency bandpass to attenuated noisy data and transform zero crossing to peaks,

129   thereby yielding semi-qualitative contourable data. Karous-Hjelt operators transform the

130   magnetic field associated with the current flow in conductive bodies to current density at the

131   depth of the conductive body (rock) causing the magnetic field to yield a 2D conductivity model

132   [6]; [13], [14].

133

134

135

136   (ii) Direct current (DC) Resistivity

137   This is a geo-electrical method which is based on the difference in electrical resistivity

138   (conductivity) of the rocks, which is a function of mineral composition, porosity, degree of water

139   saturation and fluid composition within the rocks [15]. For the purpose of this work, four

140   traverses were conducted at four different profiles where electrical sounding were conducted.

141   The equipment used measured the real (in phase) and quadrature (out of phase) components of

142   the vertical to horizontal magnetic field ratio. DC resistivity meter-SAS1000 (manufactured by

143   ABEM Co) was used to collect the resistivity data. The survey was carried out using the

144   Schlumberger configuration since it is usually designed to discriminate between electrical

145   resistivities associated with lithological and/or hydrological characteristics. In addition, it has a

146   large probing resolving power and less affected by local heterogeneity. Four DC soundings were

147   distributed in rectangular pattern to cover the area of investigation with unequal spacing. The

148   maximum spacing of half current electrode (AB/2) ranges from 1 m to 100 m, which was

149   sufficient to achieve the study purposes using Schlumberger configuration.

150   Rocks indicate a wide range of resistivities, from 10^{-6} Ωm for graphites to 10^{12} Ωm for dry

151   quartzite [16]. The form of the pores in the rocks and degree of the interconnection are among

152   the main factors which cause resistivity variation in different rocks. Fracture zones are also

153   characterized by low resistivity, since they normally contain water. The fundamental law of

154   resistivity survey is Ohm's Law that governs the flow of current in the ground. The Ohm's Law

155   in vector form can be defined as

156    $J = \sigma E$ (7)

157   where σ, the conductivity of the medium, J is the current density and E is the electric field

158   intensity. As the subsurface condition is actually inhomogeneous, the measurements provides the

159   apparent resistivity (ρ_a) of the medium which indicates the resistivity distribution of the

160   subsurface material (Fig. 2a) and can then be calculated using the current flow (I) and potential

161   difference between the electrodes:

162    $\rho_a = \mathrm{K}_g \dfrac{\Delta \phi}{I}$ (8a)

163    $\rho_a = 2\pi R \left(\dfrac{1}{r_1} - \dfrac{1}{r_2} - \dfrac{1}{r_3} + \dfrac{1}{r_4} \right)^{-1}$ (8b)
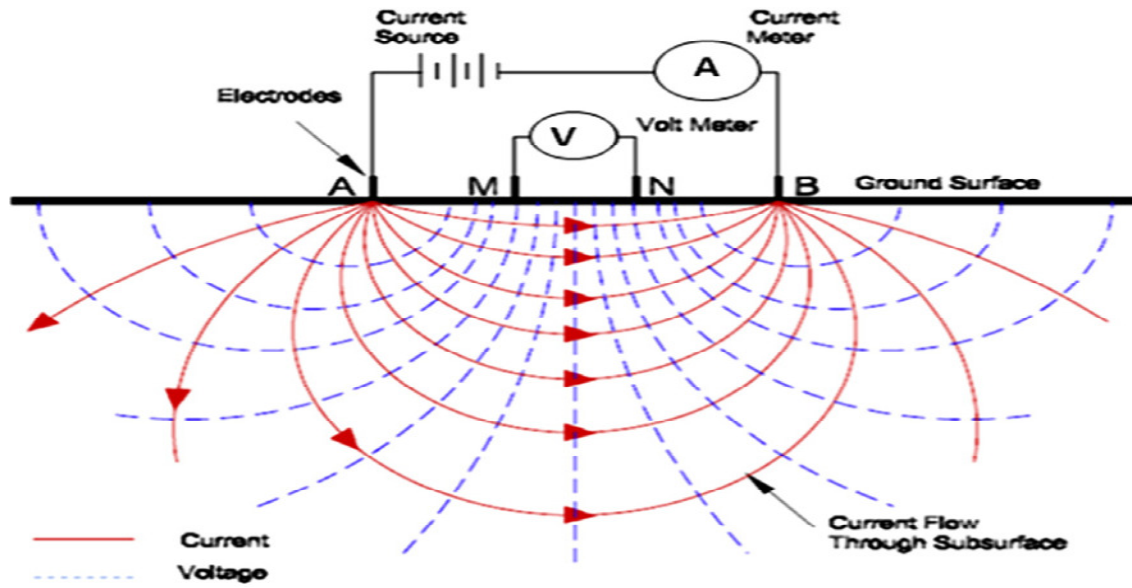
164

165 Fig. 2a: Basic measurements using the method of electrical resistivity adopted from [17]. The
166 electrical current is injected through a pair of current electrodes and the voltage difference at the
167 station is measured through a pair of receivers (potential electrodes). The parameter (K_g) in
168 equation (8a) is the geometric factor, which depends on the electrode arrays.

169 For the Schlumberger configuration, the current electrodes are spaced much further apart than the
170 potential electrodes (Fig. 2b).

171
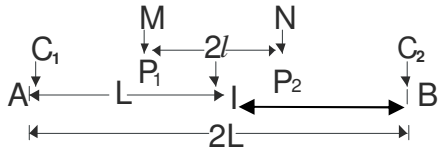
172 Fig. 2b: Schlumberger configuration

173 The Schlumberger configuration is of the form:

174
$$\rho_{sa} = 2\pi R \left(\frac{1}{r_1} - \frac{1}{r_2} - \frac{1}{r_3} + \frac{1}{r_4} \right)^{-1} \tag{9}$$

175 We have:

176
$$r_1 = L - l, r_2 = L + l, r_3 = L + l, r_4 = L - l \tag{10}$$

177
$$\rho_{sa} = 2\pi R \left(\frac{1}{L-l} - \frac{1}{L+l} - \frac{1}{L+l} + \frac{1}{L-l} \right)^{-1} \tag{11}$$

178
$$= 2\pi R\left(\frac{L+l-L+l-L+l+L+l}{L^2-l^2}\right)^{-1} = \left(\frac{4l}{L^2}\right)^{-1} \tag{12}$$

179

180 But $L \gg l$

181 $\therefore L^2 - l^2 = L^2$

182
$$\rho_{sa} = 2\pi R\frac{1}{\dfrac{4l}{L^2}} = \frac{2\pi R L^2}{4l} = \frac{\pi R L^2}{2l} \tag{13}$$

183
$$\rho_{sa} = \frac{\pi R\left(\dfrac{\text{AB}}{2}\right)^2}{\text{MN}} \tag{14}$$

184 The theoretical depth of penetration $(Z) = 0.125\text{AB}$.

185 For large value of L it may be necessary to increase l also in order to maintain a measurable

186 potential.

187 **Results and Discussion**

188 (a) VLF – EM Profiles and Map

189 The obtained VLF-EM field data were smoothed to eliminate noise and interpreted both the in-

190 phase (real) and quadrature (imaginary) using two prominent techniques outlined by [11] [12] to

191 locate the depths of concealed targets. VLF anomalies are mainly interpreted based on anomaly

192 curves and monograms e.g. [18]; [19]. Filtering and subsequent contouring of the observed

193 responses were employed to derive qualitative information about the subsurface [11]; [20]; [12].

194 Multidimensional numerical modeling and inversion were applied to determine quantitatively the

195 geometrical and physical subsurface parameters from VLF anomalies. Analytic signal approach

196 was employed because of absence of well-defined quantitative methods for interpreting VLF

197 data [21], and the Fraser filter or Hjelt filter are semi-quantitative in nature. Freely available

198 MATLAB-based software [22] was used to process the measured components of VLF-EM

199 signals. Hence, the interpretation of both the profiles and pseudo sections was basically

200 qualitative or semi quantitative.

9

201   The VLF-EM representative results of the Fraser model filtered data plots as well as Karous-

202   Hjelt filter 2-D inversion current density plots for profiles 1-4 are presented in Figs. 3(a – d) and

203   Figs. 4(a – d) respectively. High positive values indicate presence of conductive subsurface

204   structures while low or negative values are indicative of resistive formations, [23] and [24] Figs.

205   3(a – d). The 2-D inversion shows variation of apparent current density with change in

206   conductivity with depth (conductivity gradient), This is shown as regions with red patches

207   indicating areas that have been severely affected by leachate contamination (Figs. 4a, 4c and 4d).

208   (b) Schlumberger VES Iterated Curves

209   The characteristic iterated VES curves (Figs. 5a and 5b) derived from the Vertical Electrical

210   Soundings at four stations along the profile were characterised according to their responses. The

211   occurrence of contamination generates lower resistivity response as observed from VES 1, VES

212   3 and VES 4 (Table 1). VES 1 carried out in the eastern part of the dumpsite, reveals low

213   resistivity layer at a depth of 6.58 m. This implies the contamination of the low resistivity layer

214   by leachate. Also in VES 3, the western part of the dumpsite shows that soil is highly rich in

215   humus from decaying plants. As a result, the sounding has very low resistivity of 37.21 Ωm in

216   the first layer. But there was a sharp rise in the resistivity of the third layer indicating the

217   presence of a highly resistive material or an anomaly in the survey. VES 4 is also rich in humus

218   with low resistivity (40 Ωm) in the second layers have been contaminated at depth of 14.6 m.

219   However, in VES 2 performed at a reasonable distance in the southern part of the dumpsite, there
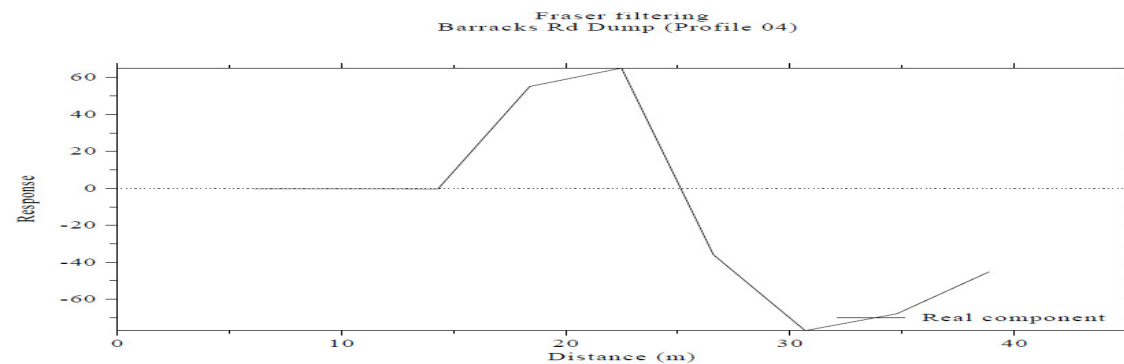
220   was no contamination.

221

222

223

224

225

226

227

228

229

230

231

232

233

234

235

236

237
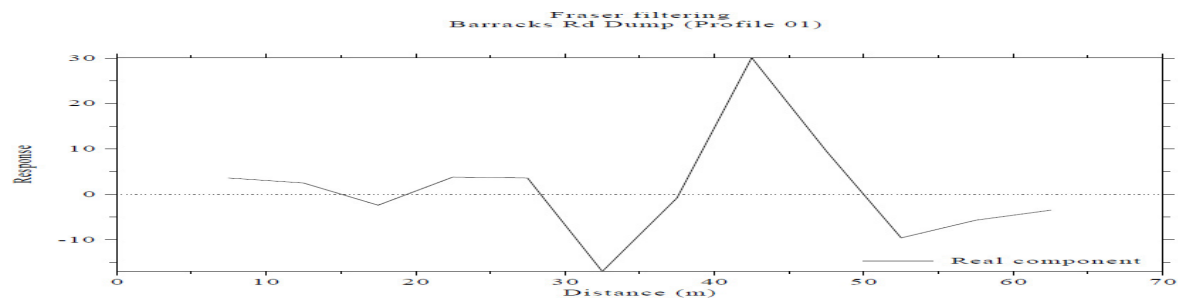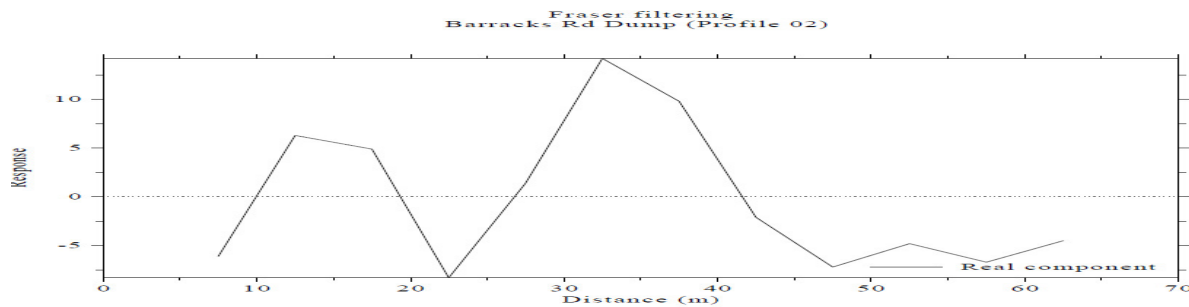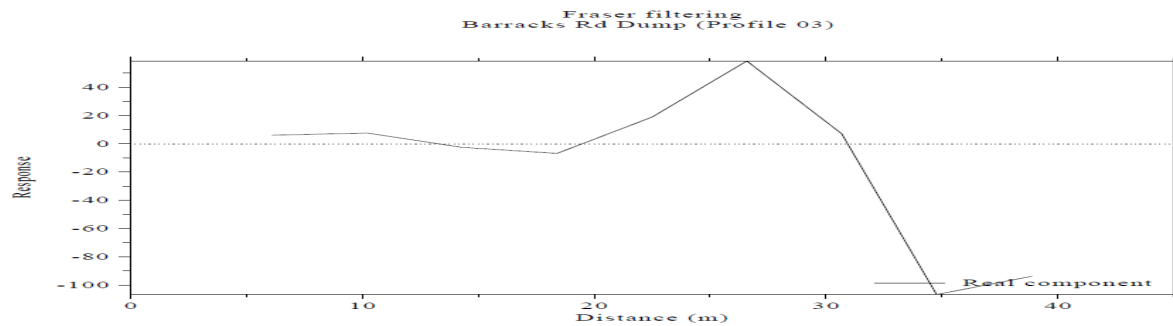
238   Fig. 3: VLF-EM Curves 3a-3d for profiles 01-04 respectively
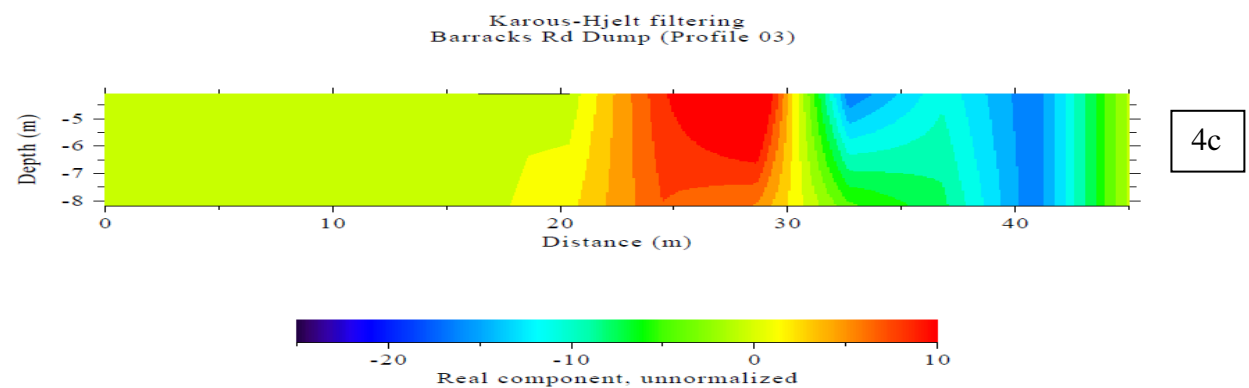
239
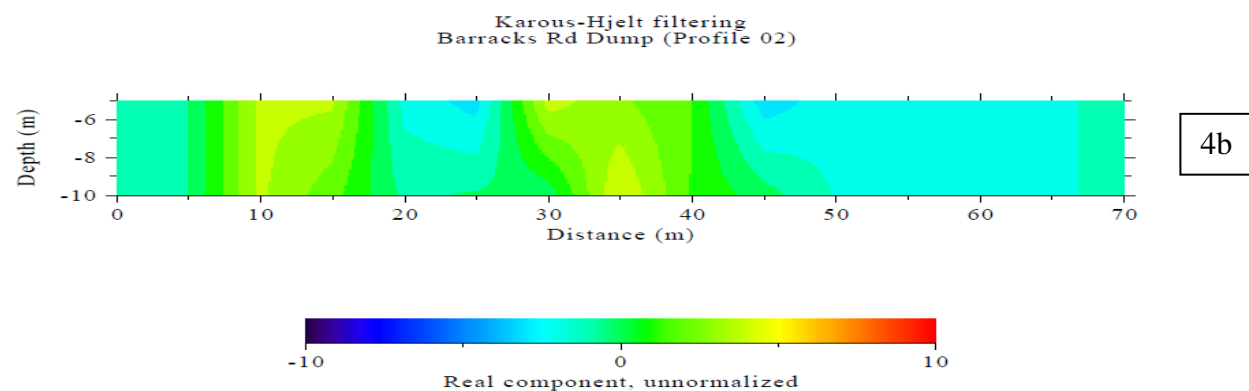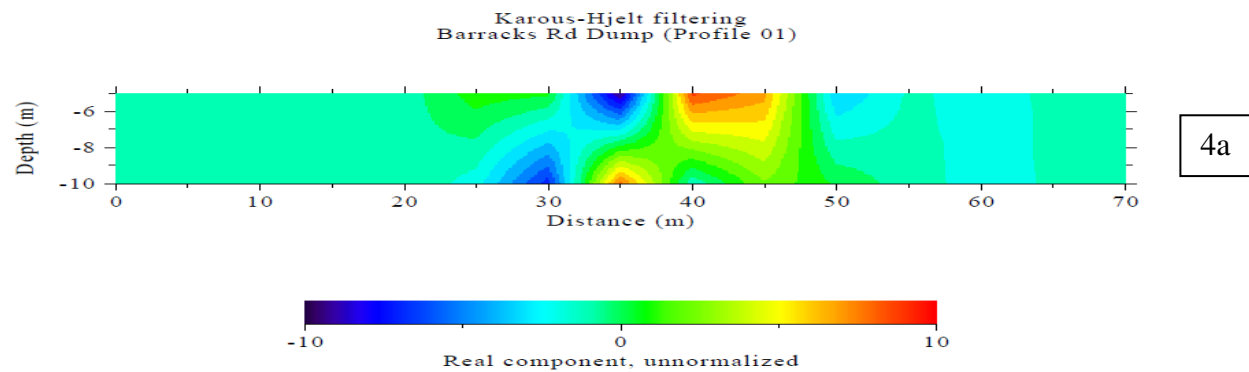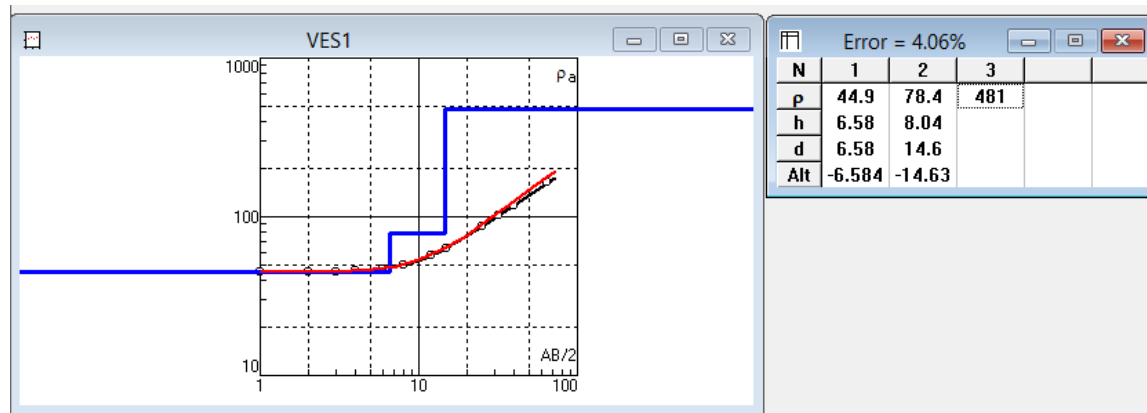
240

11

241

242
243

244

245
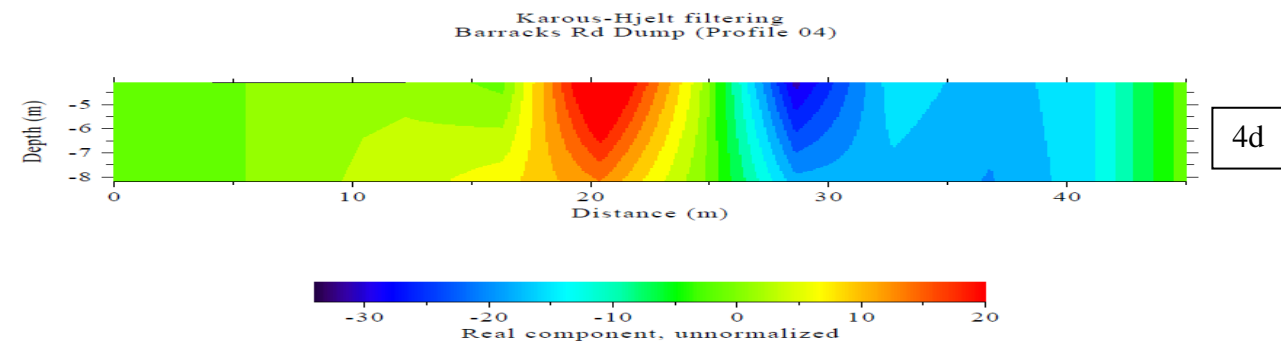
Fig. 4: 2-D inverted Karous-Hjelt model 4a-4d for profiles 01-04 respectively

247

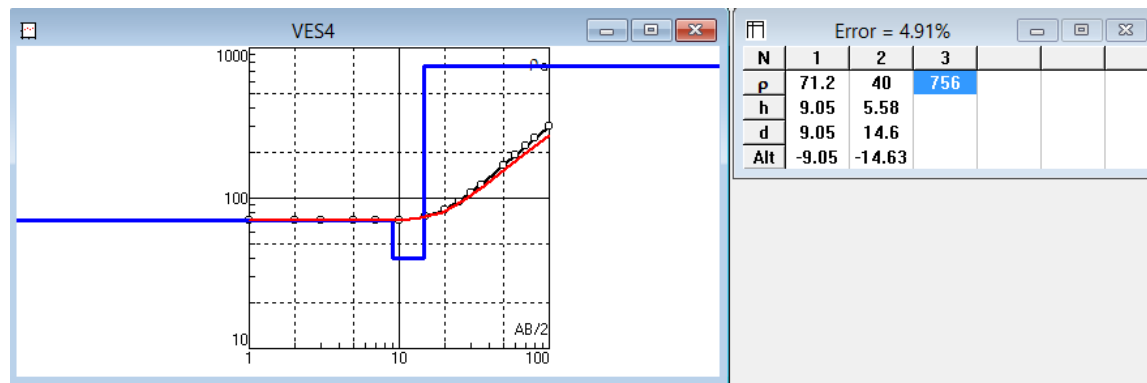248   Table 1: Smoothed iterated results from VES in police barrack road

VES Station	Layer	Resistivity (Ω)	Layer thickness (m)	Depth (m)	Curve type
VES1	ρ_1	44.9	6.58	6.58	A
	ρ_2	78.4	8.08	14.6	
	ρ_3	481	-	-	
VES2	ρ_1	82.1	0.5	0.5	A
	ρ_2	98.5	0.699	1.2	
	ρ_3	194	-	-	
VES3	ρ_1	37.21	1.08	1.08	A
	ρ_2	117.2	29.69	30.77	
	ρ_3	15269	-	-	
VES4	ρ_1	71.2	9.05	9.05	H
	ρ_2	40	5.58	14.6	
	ρ_3	756	-	-	

249

250

251   Fig. 5a: Sample of A curve type

252

253   Fig. 5b: Sample of H curve type

13

254 **Conclusion**

255 This study examined the effects of functional and an abandoned waste dumpsite on site

256 characterization located along Police Barrack Road, Ekpoma. Results from the analysis of data

257 reveal leachate generated by surface water percolating through the waste has polluted and

258 contaminated the top soil. Earth conductivity in some areas is fairly high. Layered subsurface

259 resistivity models exhibits electrically low resistive layers probably due to leachate

260 contamination. This is observed within the mean depths of 1.08 to 14.6 m (Table 1) depending

261 on the rate of decomposition of solid waste penetration. Uncontaminated areas exhibit much

262 higher resistivity.

263

264 **REFERENCES**

265 1.Allen AR, Containment Landfills: The myth of Sustainability. Eng. Geol. 2001; 60: 3-19.

266 2. Meju MA. Geoelectrical investigation of old/abandoned covered landfill sites in urban areas:

267 Model development with a genetic diagnosis approach, J. Applied Geophys. 2000; 44:115–166.

268 3. Osinowo OO, Olayinka, AI. Very low frequency electromagnetic (VLF-EM) and Electrical

269 resistivity (ER) investigation for groundwater potential evaluation in a complex geologic terrain

270 around Ijebu-ode transition zone. South Western Nigeria, Journal of Geophysics and

271 Engineering. 2012; 9(4): 74-96.

272 4. Reyment RA. Aspects of geology of Nigeria. University of Ibadan Press; 1965.

273 5. Kogbe CA. Paleogeographic History of Nigeria from Albian Times. In: Geology of Nigeria,

274 Kogbe. CA. (Ed). Elizabethan Publishers, Lagos Nigeria; 1976.

275 6. McNeill JD, Labson VF. Geological Mapping Using VLF Radio Fields Electromagnetic

276 Methods In Applied Geophysics, 1991; 521-587.

277 7. Jeng, Y, Lin, MJ, Chen, CS. A very low frequency-electromagnetic study of the geo-

278 enviromental hazardous areas in Taiwan, Enviro. Geol. 2004; 46:748-795.

279 8. Reynolds JM. An introduction to applied and Environmental geophysics. John Wiley and Sons

280 Ltd. Chichester, UK; 1997.

281 9. Kearey P Brooks M. An introduction to geophysical exploration, Blackwell, Oxford, p. 296;

282 1984.

283 10. Fischer G, Le Quang, BV, Muller, I. VLF ground surveys, a powerful tool for the study of

284 shallow two-dimensional structures, Geophys. Prosp., 1983; 31: 977-991.

14

285   11. Fraiser DC, Contouring of VLF-EM data. Geophysics. 1969. 34:958–967.

286   12. Karous M, Hjelt SE. Linear filtering of VLF dip-angle measurements. Geophys. Prospect.
287   1983; 31: 782–792.

288   13. Beamish D, Two-dimensional, regularized inversion of VLF data. J. Appl. Geophysics. 1994;
289   32: 357–374.

290   14. Beamish, D. Quantitative 2D VLF data interpretation. J. Appl. Geophys. 2000; 45: 33-47.

291   15. Kneisel C, Hauck C. Application of capacitively-coupled and DC electrical resistivity
292   imaging for mountain permafrost studies. Permafrost and Periglacial Processes. 2006; 17 (2):
293   169–177.

294   16. Parasnis DS. Principles of Applied Geophysics, 4th ed., Chapman and Hall, London; 1986.

295   17. Marescot L, Monnet R, Chapellier D. Resistivity and induced polarization surveys for slope
296   instability studies in the Swiss Alps. Eng. Geol. 2009; 98: 18–28.

297   18. Kaikkonen, P. 1979. Numerical VLF modeling. Geophys. Prosp. 27:815-834.

298   19. Saydam AS. Very low frequency electromagnetic interpretation using tilt angle and ellipticity
299   measurements. Geophysics. 1981; 46: 1594–1605.

300   20. Karous M, Hjelt SE. Determination of apparent current density from VLF measurements.
301   Finland: Department of Geophysics, University of Oulu; 1977.

302   21. Sundararajan, N. 1983. Interpretation Techniques in Geophysical Exploration Using Hilbert
303   Transform. Ph.D. Thesis, Osmania University, Hyderabad, India, pp. 191. (Unpubl.).

304   22. Sundararajan N, Babu VR, Prasad NS, Srinivas, Y. VLFPROS—A Matlab code for
305   processing of VLF-EM data. Computers & Geosciences. 2006; 32: 1806-1813.

306   23. Sharma SP, Baranwal, VC. Delineation of groundwater-bearing fracture zones in hard rock
307   area integrating VLF-EM and resistivity data. J. Appl. Geophys. 2005; 57: 155-166.

308   24. Ozegin KO, Okolie, EC. Mapping of subsurface geologic structures with Very Low
309   Frequency – Electromagnetic method (VLF – EM) in parts of Edo state, Nigeria. Nigerian
310   Journal of Physics. 2016; 27(1): 37- 44.

311